

Conf- 910414--17

UCRL-JC-104787
PREPRINT**DISCONTINUOUS FINITE-ELEMENT TRANSPORT SOLUTIONS
IN THE THICK DIFFUSION LIMIT IN CARTESIAN GEOMETRY**

Marvin L. Adams

This paper was prepared for submittal to
THE AMERICAN NUCLEAR SOCIETY INTERNATIONAL TOPICAL MEETING
Pittsburgh, PA
April 28 - May 1, 1991

January 7, 1991

Received by OSTI

FEB 19 1991

Lawrence
Livermore
National
Laboratory

This is a preprint of a paper intended for publication in a journal or proceedings. Since changes may be made before publication, this preprint is made available with the understanding that it will not be cited or reproduced without the permission of the author.

DISCLAIMER

This document was prepared as an account of work sponsored by an agency of the United States Government. Neither the United States Government nor the University of California nor any of their employees, makes any warranty, express or implied, or assumes any legal liability or responsibility for the accuracy, completeness, or usefulness of any information, apparatus, product, or process disclosed, or represents that its use would not infringe privately owned rights. Reference herein to any specific commercial products, process, or service by trade name, trademark, manufacturer, or otherwise, does not necessarily constitute or imply its endorsement, recommendation, or favoring by the United States Government or the University of California. The views and opinions of authors expressed herein do not necessarily state or reflect those of the United States Government or the University of California, and shall not be used for advertising or product endorsement purposes.

DISCONTINUOUS FINITE-ELEMENT TRANSPORT SOLUTIONS IN THE THICK DIFFUSION LIMIT IN CARTESIAN GEOMETRY

Marvin L. Adams
 Lawrence Livermore National Laboratory, L-18
 Livermore, CA 94550 (415) 422-0668

ABSTRACT

We analyze the behavior of discontinuous finite-element methods (DFEMs) for problems that contain diffusive regions. We find that in slab geometry most of these methods perform quite well, but that the same is not true in XY or XYZ geometry. In these geometries, we find that there are two distinct sets of DFEMs. Methods in one set produce unphysical solutions in diffusive regions; the others produce leading-order solutions that satisfy discretizations of the correct diffusion equation. We show that two simple properties of the finite-element weight functions are sufficient to guarantee that a DFEM belongs to the latter set. We show, however, that even these DFEMs suffer from several defects: their leading-order solutions are in general *discontinuous*, they satisfy diffusion discretizations that can be *ill-behaved*, and they may not be accurate given *boundary layers* that are not resolved by the spatial mesh. We discuss the practical significance of these defects, and we show that liberal modification of some DFEMs can eliminate the defects. We present numerical results from simple test problems; these fully agree with our analysis.

I. INTRODUCTION

Thermal-radiation transport problems of practical interest often contain optically thick, diffusive regions. Practical considerations usually force the use of a spatial mesh whose cells are thick relative to a mean-free path in such regions. We are therefore interested in the performance of numerical transport methods in diffusive regions with optically thick spatial cells. In this paper we analyze and test the behavior of a family of transport spatial discretizations, namely the discontinuous finite-element methods (DFEMs), for such problems. We find that in one-dimensional slab geometry, most DFEMs perform extremely well, provided they use *mass-matrix lumping*. (We shall describe lumping below.) We find that in two- and three-dimensional Cartesian geometries, many DFEMs fail dramatically in thick diffusive regions. We find that these DFEMs are characterized by certain properties (which we describe) of the finite-element weight functions. We show that the remaining DFEMs behave much more reasonably in diffusive regions, but that they too suffer from several defects. We introduce modifications to existing DFEMs which mitigate, and in some cases eliminate, these defects.

Our work follows from previous work by many researchers; here we summarize some of this work. Larsen, Morel and Miller¹ have used an asymptotic analysis to study the behavior of some simple slab-geometry spatial discretizations in the interior of diffusive regions. Larsen and Morel² have extended this work, analyzing the linear DFEM in slab geometry both in the interior and at the boundaries of diffusive regions. They have shown that in the interior of a thick diffusive region, a *modified* linear DFEM is very accurate. (The modification is equivalent to mass-matrix lumping, which we discuss below.) This holds even when there are transport boundary layers that are not resolved by the spatial mesh. A subsequent communication² emphasizes that the standard unlumped linear DFEM can perform poorly in diffusive slabs. Börgers, et al.³ have found that in

two-dimensional Cartesian geometry with rectangular spatial cells, the linear DFEM produces non-physical solutions in diffusive regions. Recent studies by Waring, et al.⁴ have shown that the *bilinear* DFEM method does not share the failure of the linear DFEM, at least given rectangular spatial cells and no boundary layers.

These results demonstrate a need for a better understanding of how DFEMs behave in multi-dimensional diffusive regions. Toward that end, we apply here an asymptotic diffusion-limit analysis to a very general problem. We assume Cartesian geometry, an arbitrarily-connected spatial mesh with arbitrarily-shaped cells, and finite diffusive regions upon which is incident an arbitrary angular intensity. We analyze the family of weighted-residual discontinuous finite-element methods (DFEMs) for spatially discretizing the transport equation. Perhaps our most interesting result is that we can analyze such a general problem and obtain sharp results. (We note that similar general problems have been analyzed recently.^{5,6}) We find that multidimensional DFEMs fall into two sets, one characterized by unphysical solutions in diffusive regions, and one characterized by more reasonable solutions. We show that the set to which a given DFEM belongs depends entirely on certain properties (which we specify) of the finite-element *weight functions*. We show further that even the “reasonable” DFEMs suffer from several defects. First, in the interior of a diffusive region, their leading-order solutions are in general discontinuous. This is not desirable, for the correct leading-order solution satisfies a diffusion equation and is therefore smooth. Second, the continuous components of these solutions satisfy diffusion discretizations that in general are not well-behaved. That is, the discretizations are not positive and can permit unphysical oscillations. Third, if there are transport boundary layers at the surface of a diffusive region, the leading-order DFEM solutions may be inaccurate in the interior. This can happen when the angular intensity incident upon the region is anisotropic or discontinuous. We find that mass-matrix lumping is *necessary* to obtain a robust solution, but that in two or three dimensions it is not *sufficient*. We introduce the concept of *surface-integral lumping*, and we show that it alleviates some of the defects of DFEMs. We find, however, that further modifications are needed to create a truly robust method. We introduce such modifications for the bilinear DFEM on rectangular spatial cells in two-dimensional Cartesian geometry. We provide numerical results, all of which support our theoretical claims. Finally, we offer some concluding remarks.

II. ASYMPTOTIC ANALYSIS

We begin with a very brief review of the behavior of the exact transport solution in a diffusive region. This material is taken from References [7-10]. We write the transport equation for a single energy group, assuming isotropic sources and scattering, as:

$$\Omega \cdot \nabla \Psi + \sigma_t \Psi(r, \Omega) = \frac{1}{4\pi} (\sigma_t - \sigma_a) \Phi(r) + \frac{1}{4\pi} Q(r) , \quad r \in D , \quad (1a)$$

$$\Psi(r, \Omega) = F(r, \Omega) , \quad r \in \partial D , \quad \mathbf{n} \cdot \Omega < 0 , \quad (1b)$$

where Ψ is the angular flux, Φ is the scalar flux, F is the incident angular flux, σ_t is the total cross section, σ_a is the absorption cross section, and Q is a given source. We consider the scaled transport problem:

$$\Omega \cdot \nabla \Psi + \frac{\sigma_t}{\epsilon} \Psi(r, \Omega) = \frac{1}{4\pi} \left(\frac{\sigma_t}{\epsilon} - \epsilon \sigma_a \right) \Phi(r) + \frac{\epsilon}{4\pi} Q(r) , \quad r \in D , \quad (2a)$$

$$\Psi(r, \Omega) = F(r, \Omega) , \quad r \in \partial D , \quad \mathbf{n} \cdot \Omega < 0 , \quad (2b)$$

and ask how the solution Ψ behaves as the small parameter ϵ tends toward zero. We find that to leading order in the *interior* of the diffusive region D , the solution is isotropic and satisfies a diffusion equation. This leading-order interior solution satisfies the following boundary condition:

$$\Psi(\mathbf{r}, \Omega) = \frac{1}{4\pi} \Phi(\mathbf{r}) + O(\epsilon) , \quad \mathbf{r} \text{ away from } \partial D , \quad (3a)$$

$$-\nabla \cdot \frac{1}{3\sigma_t} \nabla \Phi + \sigma_a \Phi(\mathbf{r}) = Q(\mathbf{r}) , \quad (3b)$$

$$\Phi(\mathbf{r}_s) = 2 \int_{\mathbf{n} \cdot \Omega < 0} d\Omega W(|\mathbf{n} \cdot \Omega|) F(\mathbf{r}_s, \Omega) , \quad \mathbf{r}_s \in \partial D . \quad (3c)$$

We briefly discuss this result using a simple thought problem. We imagine a mono-directional beam of particles incident upon a homogeneous region that is many mean-free paths thick and almost a pure scatterer ($\sigma_a \ll \sigma_t$). In agreement with physical intuition, Eqs. (3) say that *away from the boundaries* the solution is very nearly isotropic and very nearly satisfies the diffusion equation. We emphasize that Eq. (3c) does not describe the leading-order solution at the boundary; it describes the value obtained by smoothly *extrapolating the interior solution* to the boundary. Just inside the boundary, the solution is neither isotropic nor diffusive. In this *boundary layer*, which is on the order of a mean-free path thick, the solution may have rapid angular and spatial variations. (Figure 2 displays the solution of just such a problem.) An important question addressed by this paper is whether DFEMs can obtain accurate *interior* solutions when these boundary layers are not resolved by the spatial grid.

Equation (3c) is a Dirichlet condition equal to a weighted integral of the incoming intensity. The angular weight function W is defined in terms of Chandrasekhar's H -function for a purely scattering medium¹¹. It is reasonably well approximated by a simple polynomial:

$$W(\mu) = \frac{\sqrt{3}}{2} \mu H(\mu) ;$$

$$W(\mu) = 0.956\mu + 1.565\mu^2 \pm 0.0035 \quad = \quad \mu + 1.5\mu^2 . \quad (4)$$

When we analyze a given numerical transport method in the "diffusion limit", we find the equations that are satisfied by its leading-order solution in that limit. If these equations have no physical content, we know the numerical transport solution will be unphysical in diffusive regions. If the equations are reasonably accurate approximations to Eqs. (3), we shall conclude that the numerical transport solution will be reasonably accurate in diffusive regions.

Derivation of DFEMs

We now define the family of DFEMs that we are studying. We assume that the problem domain has been divided by a spatial grid into cells. We assume no regularity of the spatial grid. We assume that each spatial cell is polyhedron (3D), a polygon (2D), or a slab (1D). The DFEM derivation begins in cell k , where we define approximate solution functions in terms of a chosen linearly independent set of basis functions, $\{b_{kj}, 1 \leq j \leq J_k\}$:

$$\Psi(r, \Omega) \approx \psi(r, \Omega) \equiv \sum_{j=1}^{J_k} \psi_{kj}(\Omega) b_{kj}(r), \quad r \in \text{cell } k; \quad (5a)$$

$$\Phi(r) \approx \phi(r) \equiv \sum_{j=1}^{J_k} \phi_{kj} b_{kj}(r), \quad r \in \text{cell } k; \quad (5b)$$

The basis functions are assumed to be continuous within cell k but will in general be discontinuous at the boundary, ∂k , of cell k . Each b_{kj} vanishes outside of cell k . We next choose a linearly independent set of weight functions, $\{w_{ki}, 1 \leq i \leq J_k\}$, for cell k . These are also assumed to be continuous within cell k , to be discontinuous on ∂k , and to vanish outside of cell k . We multiply the transport equation (1a) by each of these weight functions and integrate over cell k . The result is J_k equations for the J_k unknowns in the cell. The i th equation is:

$$\begin{aligned} & \int_{\partial k} d^2 r w_{ki}(r) \mathbf{n}_k \cdot \Omega \psi(r, \Omega) - \int_k d^3 r \psi(r, \Omega) \Omega \cdot \nabla w_{ki} \\ & + \int_k d^3 r w_{ki} \sigma_t \psi = \frac{1}{4\pi} \int_k d^3 r w_{ki} [(\sigma_t - \sigma_a) \phi + Q] . \end{aligned} \quad (6)$$

We complete the derivation by defining cell-boundary angular fluxes as the value on the *upstream* side of the boundary:

$$\psi(r_k, \Omega) \equiv \begin{cases} \psi(r_k^+, \Omega), & \mathbf{n}_k \cdot \Omega < 0, \quad r_k \in \partial k, \\ \psi(r_k^-, \Omega), & \mathbf{n}_k \cdot \Omega < 0, \quad r_k \in \partial k, \end{cases} \quad (7)$$

where r_k^+ is just outside cell k and r_k^- is just inside. The result is a J_k by J_k matrix equation for the unknowns $\{\psi_{kj}\}$ in cell k :

$$\Omega \cdot [L_k^{surf} \Psi_k^{surf} + L_k \Psi_k] + T_k \Psi_k = \frac{1}{4\pi} (T_k - A_k) \Phi_k + \frac{1}{4\pi} q_k , \quad (8)$$

where we have defined several vectors and matrices:

$$\Psi_k = [\psi_{k1}, \dots, \psi_{kJ_k}]^t, \quad \text{etc.},$$

$$q_{ki} = \int_k d^3 r w_{ki} Q(r) ,$$

$$[L_k^{surf} \Psi_k^{surf}]_i = \int_{\partial k} d^2 r w_{ki}(r) \mathbf{n}_k \psi(r, \Omega) ,$$

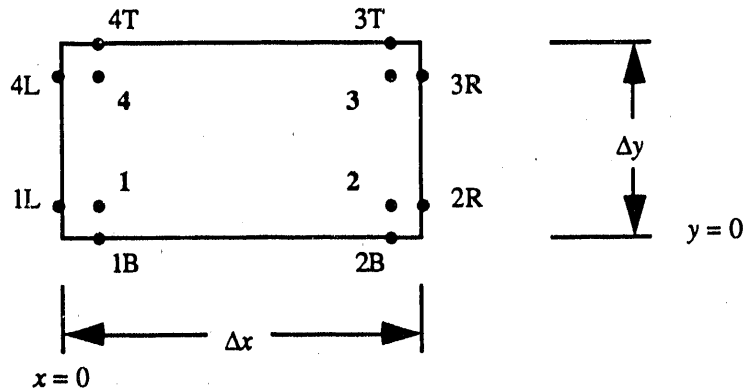
$$[\mathbf{L}_k]_{ij} = - \int_k d^3r b_{kj}(r) \nabla w_{ki} ,$$

$$[\mathbf{T}_k]_{ij} = \int_k d^3r w_{ki} \sigma_t b_{kj} , \text{ etc.}$$

Neighboring cells are coupled through their surface terms and the "upstream" definition (7). We note that the boundary condition (1a) is "naturally" included in our matrix equations; we simply recognize that

$$\psi(r_k, \Omega) = F(r_k, \Omega) \quad \text{for } r_k \in \partial D, \quad \mathbf{n}_k \cdot \Omega < 0. \quad (9)$$

We now illustrate this general method with a concrete example. We choose the bilinear DFEM on rectangular spatial cells in XY geometry. We number various points on a generic rectangle as shown below:



The numbers 1 through 4 refer to corners in the cell; L means left side, B means bottom, etc. We define bilinear basis functions:

$$b_{k1} = \frac{1-x}{\Delta x} \frac{1-y}{\Delta y}; \quad b_{k2} = \frac{x}{\Delta x} \frac{1-y}{\Delta y}; \quad b_{k3} = \frac{x}{\Delta x} \frac{y}{\Delta y}; \quad b_{k4} = \frac{1-x}{\Delta x} \frac{y}{\Delta y}, \quad (10)$$

and we use Galerkin weighting, which means $w_{ki} = b_{ki}$. We define μ to be $\mathbf{e}_x \cdot \Omega$ and η to be $\mathbf{e}_y \cdot \Omega$. For this case, Eq. (8) becomes:

$$\begin{aligned} \frac{\mu \Delta y}{6} \begin{bmatrix} -2\psi_{1L} - \psi_{4L} \\ 2\psi_{2R} + \psi_{3R} \\ \psi_{2R} + 2\psi_{3R} \\ -\psi_{1L} - 2\psi_{4L} \end{bmatrix} + \frac{\eta \Delta x}{6} \begin{bmatrix} -2\psi_{1B} - \psi_{2B} \\ -\psi_{1B} - 2\psi_{2B} \\ 2\psi_{3T} + \psi_{4T} \\ \psi_{3T} + 2\psi_{4T} \end{bmatrix} + \frac{\mu \Delta y}{12} \begin{bmatrix} 2 & 2 & 1 & 1 \\ -2 & -2 & -1 & -1 \\ 2 & -1 & -2 & -2 \\ 1 & 1 & 2 & 2 \end{bmatrix} \begin{bmatrix} \psi_1 \\ \psi_2 \\ \psi_3 \\ \psi_4 \end{bmatrix} + \frac{\eta \Delta x}{12} \begin{bmatrix} 2 & 1 & 1 & 2 \\ 1 & 2 & 2 & 1 \\ -1 & -2 & -2 & -1 \\ -2 & -1 & -1 & -2 \end{bmatrix} \begin{bmatrix} \psi_1 \\ \psi_2 \\ \psi_3 \\ \psi_4 \end{bmatrix} \\ + \frac{\sigma_t \Delta x \Delta y}{36} \begin{bmatrix} 4 & 2 & 1 & 2 \\ 2 & 4 & 2 & 1 \\ 1 & 2 & 4 & 2 \\ 2 & 1 & 2 & 4 \end{bmatrix} \begin{bmatrix} \psi_1 \\ \psi_2 \\ \psi_3 \\ \psi_4 \end{bmatrix} = \frac{(\sigma_t - \sigma_a) \Delta x \Delta y}{4\pi(36)} \begin{bmatrix} 4 & 2 & 1 & 2 \\ 2 & 4 & 2 & 1 \\ 1 & 2 & 4 & 2 \\ 2 & 1 & 2 & 4 \end{bmatrix} \begin{bmatrix} \phi_1 \\ \phi_2 \\ \phi_3 \\ \phi_4 \end{bmatrix} + \frac{\Delta x \Delta y}{4\pi(36)} \begin{bmatrix} 4 & 2 & 1 & 2 \\ 2 & 4 & 2 & 1 \\ 1 & 2 & 4 & 2 \\ 2 & 1 & 2 & 4 \end{bmatrix} \begin{bmatrix} Q_1 \\ Q_2 \\ Q_3 \\ Q_4 \end{bmatrix}. \end{aligned} \quad (11)$$

In the remainder of this paper, we shall often use these bilinear DFEM equations for illustration.

Analysis of DFEMs

We have performed an asymptotic analysis of the generic DFEM, Eq. (8), applied to the *scaled* transport problem (2). Mechanically, the scaling involves dividing the T matrices by ϵ and multiplying the A matrices by ϵ . (We note that our spatial grid remains constant as ϵ shrinks; thus, we are analyzing the “thick diffusion limit,” in which each spatial cell becomes many mean-free paths thick.) We assume an asymptotic expansion for each unknown:

$$\psi_{kj}(\Omega) = \psi_{kj}^{[0]}(\Omega) + \epsilon \psi_{kj}^{[1]}(\Omega) + \epsilon^2 \psi_{kj}^{[2]}(\Omega) + \dots , \quad (12a)$$

$$\phi_{kj} = \phi_{kj}^{[0]} + \epsilon \phi_{kj}^{[1]} + \epsilon^2 \phi_{kj}^{[2]} + \dots , \quad (12b)$$

We insert this expansion into our scaled DFEM equations, and require that the equations be satisfied for each power of ϵ . We immediately find, considering the $O(1/\epsilon)$ equations, that to leading order the DFEM angular flux is *isotropic* (equal to the scalar flux divided by 4π) everywhere:

$$\psi_{kj}^{[0]}(\Omega) = \frac{1}{4\pi} \phi_{kj}^{[0]} . \quad (13)$$

We find next (by integrating the $O(1)$ equations over angle) that the leading-order scalar flux is continuous *in a weighted-residual sense*:

$$\int_{\partial k} d^2r w_{ki}(r) [\phi^{[0]}(r_k^+) - \phi^{[0]}(r_k^-)] = 0 . \quad (14)$$

Here the scalar flux just outside the problem boundary is defined to be a weighted integral of the incident angular flux:

$$\phi^{[0]}(r_k^+) \equiv 2 \int_{\mathbf{n} \cdot \Omega < 0} d\Omega 2|\mathbf{n} \cdot \Omega| F(r_k, \Omega) , \quad r_k \in \partial D . \quad (15)$$

We pause now in our analysis to discuss the result (14), which contains a great deal of information. Equations (14) are N equations for the N leading-order scalar flux unknowns. If these equations are linearly independent, they completely determine the leading-order solution, *despite the fact that they contain no information about sources or cross sections*. Thus, if Eqs. (14) for a given DFEM are linearly independent, that DFEM’s solution will be unphysical. In fact, given vacuum boundary conditions, the leading-order solution of such a DFEM is *zero*, regardless of interior sources. On the other hand, if enough of these equations are redundant (linearly dependent), we can show that the DFEM solution will probably be reasonable.

We have determined two properties of DFEM weight functions that are sufficient to guarantee that Eqs. (14) contain redundancies. The first property is that weight functions be “local”. (It should help the reader to observe Figures 1 while trying to understand the definitions that follow.) Let us suppose there exists in a cell a linear combination of weight functions that vanishes on *all cell faces except those that meet at a given vertex*. If this is true for each vertex of each cell, we say that the DFEM’s weight functions are “local”. The second property is the existence of “mirror-image” weight functions. Let us suppose there exists a “local” linear combination of weight functions at a

given vertex of cell k , and let us define this combination to be w_{kv} . We seek a “local” linear combination of weight functions in a cell k' that is adjacent to cell k and to the given vertex; we define this combination to be $w_{k'v}$. We say that w_{kv} and $w_{k'v}$ are “mirror images” if $w_{kv}(r) \equiv w_{k'v}(r)$ for all r on the interface between cells k and k' . If such mirror images exist for all of the cells that meet at each vertex in the problem, we say that the DFEM possesses the “mirror image” property. If a DFEM possesses both the “local” and the “mirror-image” properties, there will be one redundant Eq. (14) for every vertex in the problem.

In Table 1 we examine several combinations of cell shapes and weight functions in light of Eqs. (14). Here LD refers to the linear DFEM, and BLD refers to the bilinear DFEM. We “pass” or “fail” each combination based on the two properties described above. We note that our assessments agree with previous findings^{3,4} concerning LD and BLD on rectangles; the remaining results are new. We remark that it is possible to create *slab*-geometry DFEMs that fail this test. However, this requires a very poor choice of weight functions and is unlikely to be proposed.

Equations (14) contain further information. We consider a DFEM that has the “local” and “mirror-image” properties. In this case we classify the scheme as “probably reasonable”, because its leading-order solution satisfies a discretized diffusion equation (as we show below). We now discuss the first defect that we find in these “reasonable” DFEMs. We recall that we can ignore one equation (14) at every interior vertex. We can show that the remaining equations completely determine the scalar-flux *discontinuities* throughout the problem. These equations depend only on the spatial grid, the DFEM weight and basis functions, and discontinuities in the incident partial current on the problem boundary ∂D . If the incident partial current is continuous on ∂D , then the leading-order solution of each DFEM will be continuous; otherwise, it will be discontinuous. The discontinuities, to leading order, do not depend on sources or cross sections. They are simply an unphysical artifact of standard DFEMs. We introduce now a simple modification, which we call *surface-integral lumping*, that removes this defect. The modification involves changing two of the matrices in Eq. (8):

$$[\mathbf{L}_k^{surf}]_{im}^{lump} = \delta_{ij} \sum_{i=1}^{J_k} [\mathbf{L}_k^{surf}]_{im} \quad \text{for all } m @ j; \quad (16)$$

$$[\mathbf{L}_k]_{ij}^{lump} = [\mathbf{L}_k]_{ij} + \sum_{m @ j} \left([\mathbf{L}_k^{surf}]_{im}^{lump} - [\mathbf{L}_k^{surf}]_{im} \right).$$

(We caution the reader that these formulas assume that each weight and basis function is “Cardinal”: unity at its own support point and zero at all other support points.) The notation $m @ j$ means surface points m adjacent to volume support point j . When we apply our modification to the BLD method on rectangles, Eq. (11), we obtain:

$$\begin{aligned} \frac{\mu \Delta y}{6} \begin{bmatrix} -3\psi_{1L} \\ 3\psi_{2R} \\ 3\psi_{3R} \\ -3\psi_{4L} \end{bmatrix} + \frac{\eta \Delta x}{6} \begin{bmatrix} -3\psi_{1B} \\ -3\psi_{2B} \\ 3\psi_{3T} \\ 3\psi_{4T} \end{bmatrix} + \frac{\mu \Delta y}{12} \begin{bmatrix} 4 & 2 & 1 & -1 \\ -2 & -4 & 1 & -1 \\ -1 & 1 & -4 & -2 \\ -1 & 1 & 2 & 4 \end{bmatrix} \begin{bmatrix} \psi_1 \\ \psi_2 \\ \psi_3 \\ \psi_4 \end{bmatrix} + \frac{\eta \Delta x}{12} \begin{bmatrix} 4 & -1 & 1 & ? \\ -1 & 4 & 2 & 1 \\ -1 & -2 & -4 & 1 \\ -2 & -1 & 1 & -4 \end{bmatrix} \begin{bmatrix} \psi_1 \\ \psi_2 \\ \psi_3 \\ \psi_4 \end{bmatrix} \\ + \frac{\sigma_i \Delta x \Delta y}{36} \begin{bmatrix} 4 & 2 & 1 & 2 \\ 2 & 4 & 2 & 1 \\ 1 & 2 & 4 & 2 \\ 2 & 1 & 2 & 4 \end{bmatrix} \begin{bmatrix} \psi_1 \\ \psi_2 \\ \psi_3 \\ \psi_4 \end{bmatrix} = \frac{(\sigma_i - \sigma_a) \Delta x \Delta y}{4\pi(36)} \begin{bmatrix} 4 & 2 & 1 & 2 \\ 2 & 4 & 2 & 1 \\ 1 & 2 & 4 & 2 \\ 2 & 1 & 2 & 4 \end{bmatrix} \begin{bmatrix} \phi_1 \\ \phi_2 \\ \phi_3 \\ \phi_4 \end{bmatrix} + \frac{\Delta x \Delta y}{4\pi(36)} \begin{bmatrix} 4 & 2 & 1 & 2 \\ 2 & 4 & 2 & 1 \\ 1 & 2 & 4 & 2 \\ 2 & 1 & 2 & 4 \end{bmatrix} \begin{bmatrix} Q_1 \\ Q_2 \\ Q_3 \\ Q_4 \end{bmatrix}. \end{aligned} \quad (17)$$

The physical content of our modification is that communication between neighboring cells has been made *local*. The only surface quantities first row of Eqs. (17), for example, are ψ_{kIL} and ψ_{kIB} ;

“far neighbors” ψ_{k4L} and ψ_{k2B} are no longer present. The mathematical result is that Eqs. (14) are replaced by simpler equations, each of which involves discontinuities at a *single vertex*. We now find that the discontinuities vanish at each interior vertex. We remark that our modification has no effect on slab-geometry DFEMs.

At this point we have not proceeded very far into our asymptotic analysis. Already we have learned more, however, than we could have learned from analyzing specific DFEMs in specific geometries on specific spatial meshes. First, we have obtained a simple test for classifying any given DFEM as “a failure” or as “probably reasonable”. Second, we have identified a defect present in all of the “reasonable” DFEMs. Third, we have introduced a modification that eliminates this defect. Finally, we have gained useful insights into what makes DFEMs work or not work in the thick diffusion limit.

We now continue our asymptotic analysis. After some algebra, we quickly find another defect in standard DFEMs: unresolved boundary layers will be treated poorly unless we employ *mass-matrix lumping*. This is a generalization of the result found by Larsen and Morel² for the slab-geometry linear DFEM. (Mass-matrix lumping is one way to obtain the “ $\theta=1$ ” scheme of their paper.) Mass lumping changes the T and A matrices in our DFEMs:

$$[T_k]_{ij}^{lump} = \delta_{ij} \sum_{i=1}^{J_k} [T_k]_{ij} ; \quad [A_k]_{ij}^{lump} = \delta_{ij} \sum_{i=1}^{J_k} [A_k]_{ij} . \quad (18)$$

(We have again assumed Cardinal weight and basis functions.) A similar change is made to the source term. The physical content of this modification is that the collision and source terms have been made more *local*. With both mass-matrix and surface-integral lumping, our BLD scheme on rectangles becomes:

$$\begin{aligned} \frac{\mu \Delta y}{6} \begin{bmatrix} -3\psi_{1L} \\ 3\psi_{2R} \\ 3\psi_{3R} \\ -3\psi_{4L} \end{bmatrix} + \frac{\eta \Delta x}{6} \begin{bmatrix} -3\psi_{1B} \\ -3\psi_{2B} \\ 3\psi_{3T} \\ 3\psi_{4T} \end{bmatrix} + \frac{\mu \Delta y}{12} \begin{bmatrix} 4 & 2 & 1 & -1 \\ -2 & -4 & 1 & -1 \\ -1 & 1 & -4 & -2 \\ -1 & 1 & 2 & 4 \end{bmatrix} \begin{bmatrix} \psi_1 \\ \psi_2 \\ \psi_3 \\ \psi_4 \end{bmatrix} + \frac{\eta \Delta x}{12} \begin{bmatrix} 4 & -1 & 1 & 2 \\ -1 & 4 & 2 & 1 \\ -1 & -2 & -4 & 1 \\ -2 & -1 & 1 & -4 \end{bmatrix} \begin{bmatrix} \psi_1 \\ \psi_2 \\ \psi_3 \\ \psi_4 \end{bmatrix} \\ + \frac{\sigma_i \Delta x \Delta y}{4} \begin{bmatrix} \psi_1 \\ \psi_2 \\ \psi_3 \\ \psi_4 \end{bmatrix} = \frac{(\sigma_i - \sigma_a) \Delta x \Delta y}{4\pi(4)} \begin{bmatrix} \phi_1 \\ \phi_2 \\ \phi_3 \\ \phi_4 \end{bmatrix} + \frac{\Delta x \Delta y}{4\pi(4)} \begin{bmatrix} Q_1 \\ Q_2 \\ Q_3 \\ Q_4 \end{bmatrix} . \end{aligned} \quad (19)$$

We now continue our analysis, considering DFEMs with both kinds of lumping. We find that the leading-order interior solution satisfies a discrete diffusion equation. We let pq denote some vertex that is at least two cells away from the boundary. Then we find that the scalar flux at pq is coupled to the scalar fluxes at all support points in all the cells that touch pq . Given our modified BLD method on rectangles, the result is a nine-point diffusion equation. For the simple case of Δx , Δy , σ_i , and σ_a constant, this becomes:

$$\begin{aligned} \frac{1}{18\sigma_i \Delta x \Delta y} \left\{ \phi_{p,q} [8a + 8a^{-1}] - [\phi_{p+1,q+1} + \phi_{p+1,q-1} + \phi_{p-1,q-1} + \phi_{p-1,q+1}] [a + a^{-1}] \right. \\ \left. - [\phi_{p+1,q} + \phi_{p-1,q}] [4a - 2a^{-1}] - [\phi_{p,q+1} + \phi_{p,q-1}] [4a^{-1} - 2a] \right\} + \sigma_a \phi_{p,q} = Q_{p,q} , \quad (20) \end{aligned}$$

where (p,q) is the index of some interior vertex, $(p+1,q)$ is the vertex to the right, $(p,q+1)$ is the vertex above, etc., and a is the ratio $\Delta x/\Delta y$.

A close look at this result reveals another DFEM defect. The term that couples a point to its horizontal or vertical neighbor can vanish or have the wrong sign if $\Delta x \neq \Delta y$ (which means $a \neq 1$). This can lead to unphysical oscillations and negative values in the leading-order solution.

The above discussion concerns vertices that are two or more cells away from the boundary; thus, boundary conditions did not come into play. At a vertex that is only one cell away from the boundary, the equations satisfied by the leading-order solution do depend on the transport boundary condition. These equations reveal how a given DFEM performs in the presence of unresolved boundary layers. We assume, for simplicity of presentation, that the incident angular flux is spatially continuous across the boundary, ∂D , of the diffusive region. Then we find that at each boundary vertex, two different quantities appear in our equations. Each is a weighted angular integral of the incident intensity:

$$\phi^{[0]}(r_k^+) \equiv 2 \int_{\mathbf{n} \cdot \Omega < 0} d\Omega 2|\mathbf{n} \cdot \Omega| F(r_k, \Omega) , \quad r_k \in \partial D ; \quad (21a)$$

$$\Phi(r_k^+) \equiv 2 \int_{\mathbf{n} \cdot \Omega < 0} d\Omega \left(\mathbf{n} \cdot \mathbf{n} \cdot \Omega + \frac{3}{2} \Omega(\mathbf{n} \cdot \Omega) \right) F(r_k, \Omega) , \quad r_k \in \partial D . \quad (21b)$$

We recall that the exact leading-order interior solution extrapolates to the boundary condition (3c). We note that $\phi^{[0]}$ is not always an accurate approximation to Eq. (3c), for $2|\mathbf{n} \cdot \Omega|$ is not always an accurate approximation to $W(|\mathbf{n} \cdot \Omega|)$. However, we recognize that the normal component of Φ , $\mathbf{n} \cdot \Phi$, is an accurate approximation to Eq. (3c) [see Eq. (4)]. Thus, if the interior-vertex equations contain only $\mathbf{n} \cdot \Phi$ quantities at boundaries, then the interior solution extrapolates to an accurate value at boundaries. This is precisely what happens in slab geometry, given mass-matrix lumping. However, in 2D and 3D the DFEM equations include the normal component of Φ , the non-normal components of Φ , and $\phi^{[0]}$. The precise combination of these quantities to which the leading-order interior solution extrapolates depends on the grid, weight functions, and basis functions. However, it appears that significant inaccuracies are possible. Thus, we find that in the thick diffusion limit, multidimensional DFEMs do not retain the excellent boundary-layer behavior of the slab-geometry DFEMs.

For the specific case of BLD on rectangles, we have developed yet another modification that removes all identified diffusion-limit defects. We modify the gradient matrix \mathbf{L}_k to make the method's gradient approximation more *local*. The resulting scheme is:

$$\begin{aligned} \frac{\mu \Delta y}{2} \begin{bmatrix} -\psi_{1L} \\ \psi_{2R} \\ \psi_{3R} \\ -\psi_{4L} \end{bmatrix} + \frac{\eta \Delta x}{2} \begin{bmatrix} -\psi_{1B} \\ -\psi_{2B} \\ \psi_{3T} \\ \psi_{4T} \end{bmatrix} + \frac{\mu \Delta y}{4} \begin{bmatrix} +\psi_1 + \psi_2 \\ -\psi_1 - \psi_2 \\ -\psi_3 - \psi_4 \\ +\psi_3 + \psi_4 \end{bmatrix} + \frac{\eta \Delta x}{4} \begin{bmatrix} +\psi_1 + \psi_4 \\ +\psi_2 + \psi_3 \\ -\psi_2 - \psi_3 \\ -\psi_1 - \psi_4 \end{bmatrix} \\ + \frac{\sigma_i \Delta x \Delta y}{4} \begin{bmatrix} \psi_1 \\ \psi_2 \\ \psi_3 \\ \psi_4 \end{bmatrix} = \frac{(\sigma_i - \sigma_a) \Delta x \Delta y}{4\pi(4)} \begin{bmatrix} \phi_1 \\ \phi_2 \\ \phi_3 \\ \phi_4 \end{bmatrix} + \frac{\Delta x \Delta y}{4\pi(4)} \begin{bmatrix} Q_1 \\ Q_2 \\ Q_3 \\ Q_4 \end{bmatrix} . \end{aligned} \quad (22)$$

This scheme has many nice properties in the thick diffusion limit. The interior solution now satisfies a *five-point*, instead of the previous *nine-point*, differencing:

$$\frac{1}{3\sigma_a \Delta x \Delta y} \left\{ \phi_{p,q} [2a + 2a^{-1}] - [\phi_{p+1,q} + \phi_{p-1,q}] [a^{-1}] - [\phi_{p,q+1} + \phi_{p,q-1}] [a] \right\} + \sigma_a \phi_{p,q} = Q_{p,q} , \quad (23)$$

This differencing is positive and non-oscillatory. Furthermore, at every boundary vertex the interior solution extrapolates to $n\Phi$, where Φ is given by Eq. (21b). Thus, our heavily-modified bilinear DFEM performs exactly as well on rectangles as the mass-lumped linear DFEM does in slabs. We have not discovered how to extend this performance to arbitrary DFEMs or arbitrary grids.

III. NUMERICAL RESULTS

We consider first a homogeneous, purely-scattering ($\sigma_a=0$) slab 1000 mean-free paths thick. Incident upon the left face is a mono-directional beam at a cosine of $\mu_{inc} \approx 0.095$. We solve this problem with the S_{16} Gauss-Legendre quadrature set, which has an ordinate at the angle of the incident beam. We obtain a reference solution with an extremely fine spatial grid using the (mass-matrix-lumped) linear DFEM (LD). We also obtain a solution using LD with 10 equally-spaced cells. The reference solution is plotted as a heavy line in Fig. 2. We direct attention to the rapid variation at the left boundary, where the solution is plotted as an almost vertical line. We note that away from this boundary layer the interior solution is linear, and that it extrapolates to a boundary value of approximately $2[W(\mu_{inc})] \approx 0.21$. The coarse-mesh result is also linear in the interior, and it extrapolates to approximately $2[\mu_{inc} + 1.5\mu_{inc}^2] \approx 0.22$ at the boundary. All of this is predicted by the asymptotic analysis. The actual LD solution at the left boundary is approximately $2[2\mu_{inc}] = 0.38$; again, this is predicted by the analysis. We have generated all of our solutions using the DFEM diffusion-synthetic acceleration (DSA) iteration method that is described in reference [12].

We consider next a homogeneous square with a constant isotropic source and vacuum boundaries. The square is 1 by 1; we place on it a 20×20 uniform spatial mesh. We consider two test problems, each of which has cross sections and sources of the form $\sigma_t = 1/\varepsilon$, $\sigma_a = \varepsilon$, and $Q = \varepsilon$. We choose $\varepsilon = 10^{-2}$ for the first problem and $\varepsilon = 10^{-5}$ for the second. We solve each problem with the standard linear and bilinear DFEMs using the S_8 level-symmetric quadrature set; we present the results in Figs. 3 and 4. We also numerically solve the diffusion problem (3) that is satisfied by the exact transport solution in the limit as ε approaches zero; we also display this result in Fig. 4. (We take from reference [3] the figures showing the linear and diffusion solutions.) We note that the linear DFEM solution approaches zero as the problem gets more diffusive, as predicted by our analysis of Eqs. (14). We further note that the bilinear DFEM solution is very accurate; again, this is predicted by our analysis, for this problem has none of the characteristics that expose the defects of such "reasonable" DFEMs. (The incident angular flux is continuous, the grid cells are square, and there are no boundary layers.) Again, we have generated all of our results using the DFEM-DSA iteration scheme of reference [12].

Finally, we consider a homogeneous square problem that we have designed to highlight the defects in standard DFEMs. The problem, which is depicted in Fig. 5, has a slightly nonuniform spatial grid containing some cells with a 5:3 aspect ratio. The boundary condition is designed to produce boundary layers. On part of the boundary, *alternating* cells are exposed to a mono-directional beam incident at a grazing angle; remaining cells are exposed to a vacuum. In Figs. 6 we compare contour plots of two solutions to the problem. We note that the mass-matrix-lumped bilinear DFEM solution exhibits discontinuities and oscillations in the interior, just as our analysis predicts. Our contour plots do not show it, but the method also produces a negative solution along much of the vacuum boundary. We obtain similar results using a uniform square grid. In contrast, our

heavily-modified bilinear DFEM solution is smooth, as the correct (diffusion) solution must be, and it produces no negative values. We point out that both methods produce inaccurate solutions in the cells adjacent to non-vacuum boundaries. This behavior is identical to that seen in the slab-geometry mass-lumped LD method (see Fig. 2). Again, the asymptotic analysis precisely predicts all of this behavior.

IV. CONCLUSIONS

We have analyzed the behavior of discontinuous finite-element methods (DFEMs) applied to the transport equation, for problems that contain thick diffusive regions. Our analysis holds for an entire family of DFEMs, in 3D Cartesian geometry on an arbitrary spatial mesh. We have found that some DFEMs fail dramatically in thick diffusive problems, and we have found specific properties of the finite-element weight functions that lead to this failure. We have also found that some DFEMs behave reasonably in such problems, in the sense that their leading-order interior solutions satisfy discretizations of a diffusion equation. We have found that these reasonable DFEMs suffer from several defects, and that these methods must be significantly modified if they are to be free of such defects. We have found that mass-matrix lumping is one modification that is required. We have introduced a second modification, which we call surface-integral lumping, that is also required. We have found that these modifications lead to improved solution behavior, but that further modification is needed if a truly robust method is to be obtained. We have introduced such a modification for the bilinear DFEM on rectangles in two dimensions, and we have found that the new method is quite superior to unmodified and partially-modified methods. We have demonstrated the validity of our theoretical results with several numerical tests.

Our study has taken place in Cartesian coordinates, in which the transport equation is somewhat simpler than it is in curvilinear coordinates. We note that Palmer and Adams¹³ have performed a similar study in one-dimensional spherical geometry. We expect to extend this to one- and two-dimensional cylindrical geometries in the near future.

Our experience with multidimensional DFEMs in the thick diffusion limit has not been entirely encouraging. As we have explained, these methods possess several defects. We are not prepared to condemn DFEMs for diffusive problems; it may be that their defects will not seriously degrade their performance on an interesting set of such problems. However, in pursuit of a truly robust multidimensional method, we are developing a new spatial discretization. The two-dimensional Cartesian version of our present attempt is introduced in reference [14]. It is interesting that when spatial cells are rectangular, this new method reduces to our heavily-modified BLD scheme.

Our analysis has taken place on transport equations with spatial discretization but no angular discretization. This keeps the analysis simple, and serves to isolate errors that are due to the spatial discretization scheme. It will hold for any reasonable angular discretization in the limit of fine angular resolution. We note for completeness that recent work by Jin and Levermore¹⁵ shows that angular discretizations can also introduce errors in the boundary condition satisfied by the leading-order solution in diffusive regions.

ACKNOWLEDGEMENTS

We thank Edward Larsen, Gerald Pomraning, and Paul Nowak for many helpful discussions. This work was performed under the auspices of the U.S. Department of Energy by Lawrence Livermore National Laboratory under Contract #W-7405-Eng-48.

REFERENCES

1. E.W. Larsen, J.E. Morel, and W.F. Miller, Jr., "Asymptotic Solutions of Numerical Transport Problems in Optically Thick, Diffusive Regimes," *J. Comput. Physics*, **69**, p. 263 (1987).
2. E.W. Larsen and J.E. Morel, "Asymptotic Solutions of Numerical Transport Problems in Optically Thick, Diffusive Regimes II," *J. Comput. Physics*, **83**, p. 212 (1989). [See also the corrigendum to appear in *J. Comput. Physics*.]
3. C. Börgers, E.W. Larsen, and M.L. Adams, "The Asymptotic Diffusion Limit of a Linear Discontinuous Discretization of a Two-Dimensional Transport Equation", *J. Comput. Physics*, to appear.
4. T.A. Wareing, E.W. Larsen, and M.L. Adams, "Diffusion Accelerated Discontinuous Finite Element Schemes for the S_N Equations in Slab and X,Y Geometries," submitted to this conference (1991).
5. M.L. Adams, "Even-Parity Finite-Element Transport Methods in the Diffusion Limit," *Progress in Nuclear Energy*, submitted (1990).
6. M.L. Adams, "Even- and Odd-Parity Finite-Element Transport Solutions in the Thick Diffusion Limit," these proceedings (1991).
7. E.W. Larsen and J.B. Keller, "Asymptotic Solution of Neutron Transport Problems for Small Mean Free Paths," *J. Math. Physics* **15**, 75-81 (1974).
8. G.J. Habetler and B.J. Matkowsky, "Uniform Asymptotic Expansions in Transport Theory with Small Mean Free Paths, and the Diffusion Approximation," *J. Math. Physics* **16**, 846-854 (1975).
9. E.W. Larsen, "Diffusion Theory as an Asymptotic Limit of Transport Theory for Nearly Critical Systems with Small Mean Free Paths," *Annals of Nuclear Energy* **7**, 249-255 (1980).
10. F. Malgavi and G.C. Pomraning, "Initial and Boundary Conditions for Diffusive Linear Transport Problems," to appear in *J. Math. Physics* (1990).
11. S. Chandrasekhar, *Radiative Transfer*, Dover, New York (1960).
12. M.L. Adams, "Diffusion-Synthetic Acceleration of Discontinuous Finite-Element Transport Iterations," *Nucl. Sci. Eng.*, submitted.
13. T.S. Palmer and M.L. Adams, "Analysis of Spherical Geometry Finite Element Transport Solutions in the Thick Diffusion Limit," these proceedings (1991).
14. M.L. Adams, "A New Transport Discretization Scheme for Arbitrary Spatial Meshes in XY Geometry," these proceedings (1991).
15. S. Jin and C.D. Levermore, "The Discrete-Ordinate Method in Diffusive Regimes," submitted (1991).

Table 1. Performance of specific DFEMs given specific spatial cell shapes in two dimensions.

Cell Shape	Weight-Function Space	Comments
	$\{1, x, y\}$ (LD)	reasonable
	$\{1, x, y\}$ (LD)	fails
	$\{1, x, y, xy\}$ (BLD)	reasonable
	$\{1, x, y, xy\}$ (BLD)	fails
	$\{1, a, b, ab\}$ (BLD in mapped coords.)	reasonable
	?	all previously-proposed DFEMs fail on arbitrary polygons

Figures 1. A “local” weight function (left); two “mirror-image” weight functions (right).

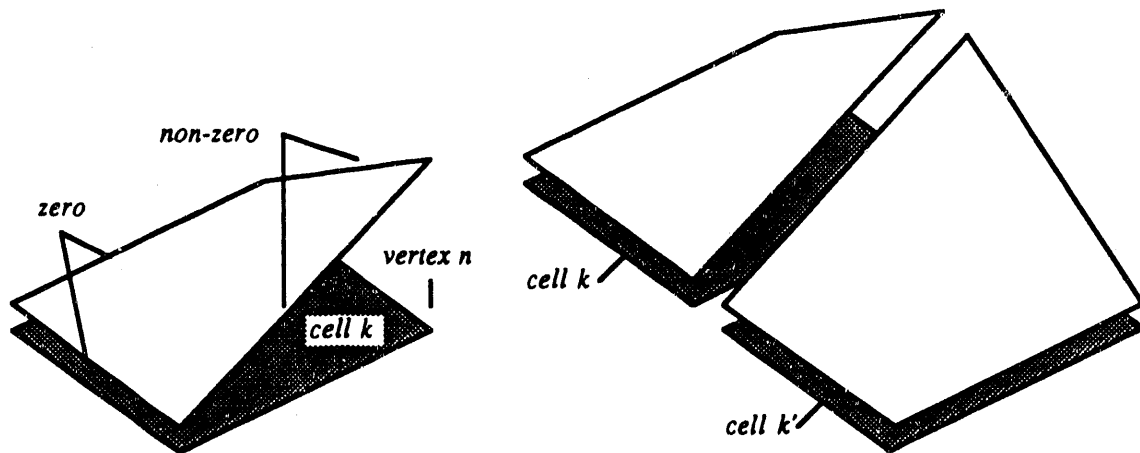
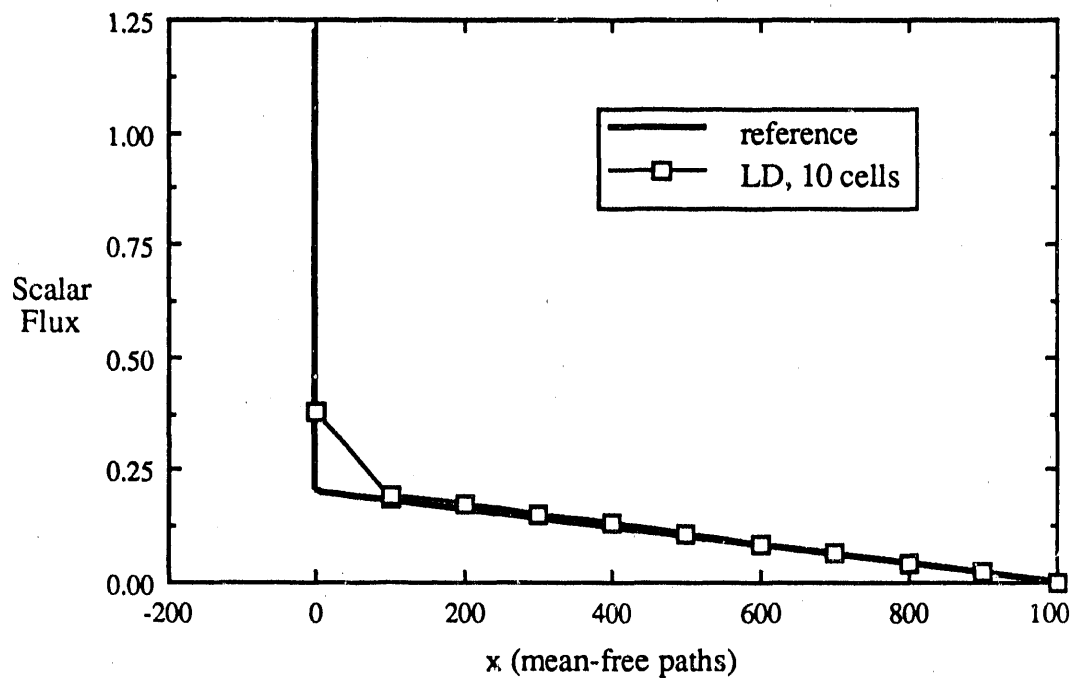
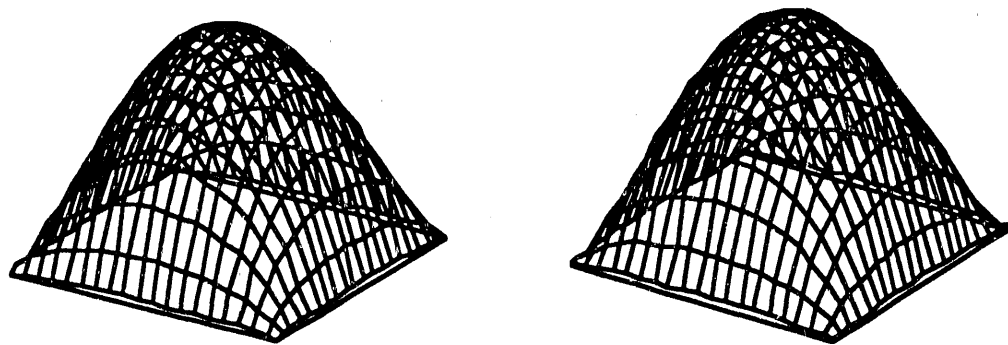


Figure 2. Reference and LD solutions of slab test problem.



Figures 3. LD (left) and BLD solutions of simple XY test problem, $\epsilon = 10^{-2}$.



Figures 4. LD (left), BLD (middle), and diffusion solutions, $\epsilon = 10^{-5}$

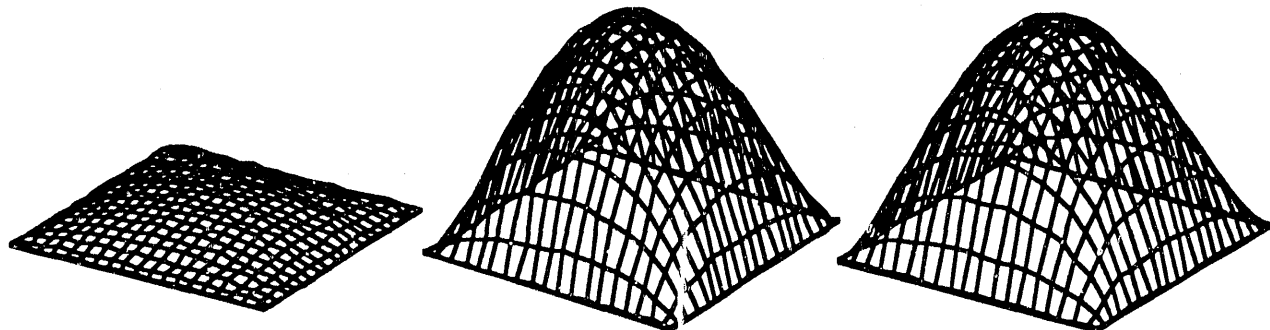
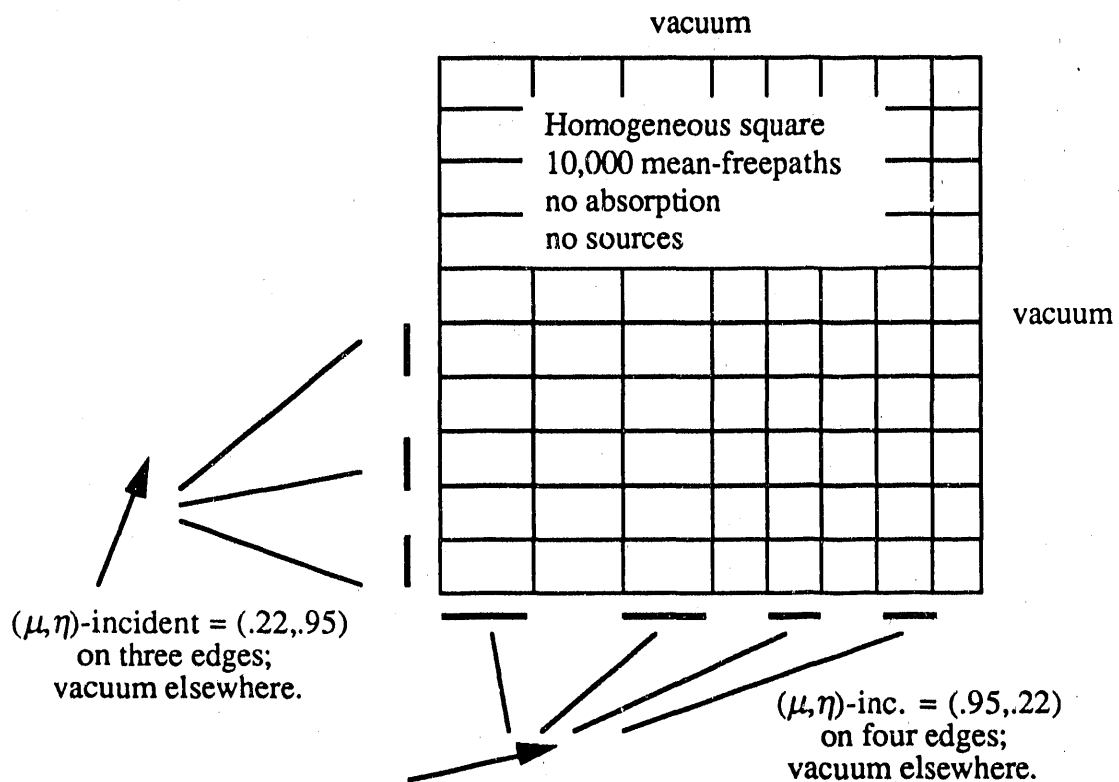
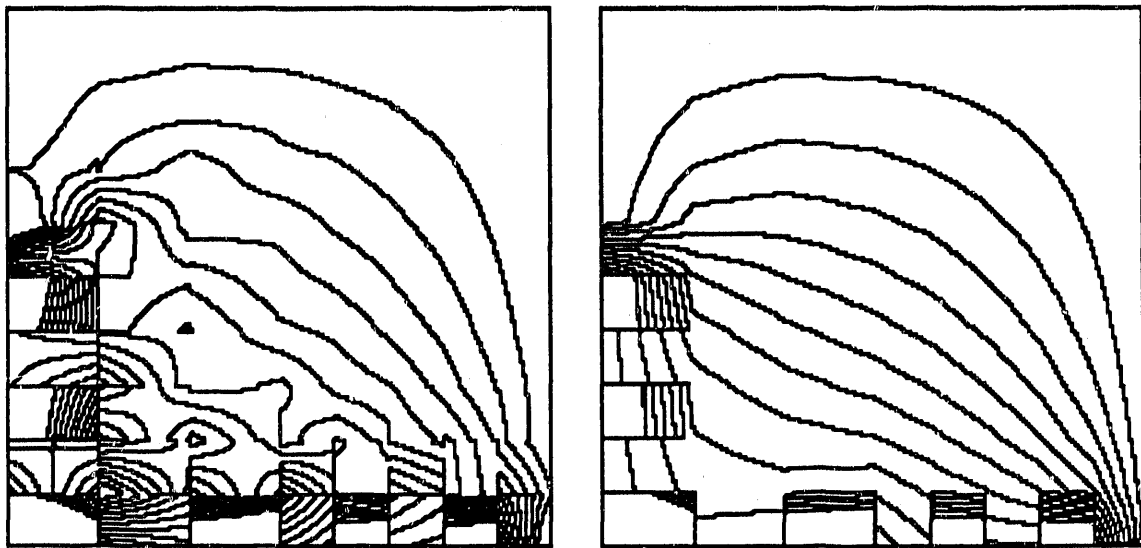


Figure 5. Difficult XY diffusion-limit problem.



Figures 6. Mass-lumped BLD (left) and new BLD solutions to the above problem.
Contours range from 0.05 to 0.70 in increments of 0.05.



END

DATE FILMED

03/05/91

